Molecular Biology of the Cell
Vol. 9, 671–683, March 1998

PDZ Motifs in PTP-BL and RIL Bind to Internal Protein Segments in the LIM Domain Protein RIL

Edwin Cuppen, Herlinde Gerrits, Barry Pepers, Bé Wieringa, and Wiljan Hendriks*

Department of Cell Biology and Histology, Institute of Cellular Signaling, University of Nijmegen, the Netherlands

Submitted December 10, 1997; Accepted January 9, 1998
Monitoring Editor: Carl-Hendrik Heldin

The specificity of protein–protein interactions in cellular signaling cascades is dependent on the sequence and intramolecular location of distinct amino acid motifs. We used the two-hybrid interaction trap to identify proteins that can associate with the PDZ motif-rich segment in the protein tyrosine phosphatase PTP-BL. A specific interaction was found with the Lin-11, Isl-1, Mec-3 (LIM) domain containing protein RIL. More detailed analysis demonstrated that the binding specificity resides in the second and fourth PDZ motif of PTP-BL and the LIM domain in RIL. Immunohistochemistry on various mouse tissues revealed a submembranous colocalization of PTP-BL and RIL in epithelial cells. Remarkably, there is also an N-terminal PDZ motif in RIL itself that can bind to the RIL-LIM domain. We demonstrate here that the RIL-LIM domain can be phosphorylated on tyrosine in vitro and in vivo and can be dephosphorylated in vitro by the PTPase domain of PTP-BL. Our data point to the presence of a double PDZ-binding interface on the RIL-LIM domain and suggest tyrosine phosphorylation as a regulatory mechanism for LIM-PDZ associations in the assembly of multiprotein complexes. These findings are in line with an important role of PDZ-mediated interactions in the shaping and organization of submembranous microenvironments of polarized cells.

INTRODUCTION

Extracellular signals initiate signaling cascades within the cell by activating distinct receptor molecules on the cell surface. Signals are then propagated and amplified via specific cytosolic proteins or second messengers and ultimately are translated in specific cellular responses (Songyang and Cantley, 1995). Separate cascades in this complex signaling network depend on specific protein–protein interactions, which are mediated by different protein motifs such as SH2, SH3, PID/PTB, and PH domains (Cohen *et al.*, 1995; Pawson, 1995; Lemmon *et al.*, 1996). Reversible tyrosine phosphorylation plays an important regulatory role in signal transduction events (Hunter, 1995); for example, SH2 and PID–PTB interactions are critically dependent on this type of modification. The role of protein tyrosine kinases in these processes has been studied extensively; target molecules have been identified and a broad range of cellular effects have been characterized. In contrast, relatively little is known about the role of protein tyrosine phosphatases (PTPases), although many different PTPase family members have been isolated over the past years. PTPases contain one or two catalytic domains and a bewildering variety of protein motifs, which may serve to target the enzymes to restricted microcompartments and specific substrates within the cell (Mauro and Dixon, 1994). The current challenge is to obtain a better understanding of these features and identify subcellular compartments and binding proteins.

Mouse PTP-BL (Hendriks *et al.*, 1995) or RIP (Chida *et al.*, 1995) is a large cytosolic PTPase (Figure 1A) containing a single catalytic tyrosine phosphatase domain and protein motifs that show similarities to both submembranous proteins and known tumor suppres-

* Corresponding author: Dr. W.J.A.J. Hendriks, Department of Cell Biology and Histology, Institute of Cellular Signaling, University of Nijmegen, P.O. Box 9101, 6500 HB Nijmegen, the Netherlands.

sor gene products. The human homologue of this protein has been termed PTP-BAS (Maekawa *et al.*, 1994), hPTP1E (Banville *et al.*, 1994), PTPL1 (Saras *et al.*, 1994), and FAP-1 (Sato *et al.*, 1995). Chromosomal localization of PTP-BAS placed the gene on 4q21, a region for which various cytogenetic abnormalities in human tumors have been reported (Inazawa *et al.*, 1996; van den Maagdenberg *et al.*, 1996). The PTP-BL polypeptide is split up in several distinct segments. Its N terminus is subject to alternative splicing (Chida *et al.*, 1995; our unpublished observations) and contains a putative leucine zipper motif (Saras *et al.*, 1994), which may be involved in homo- or heterodimerization of the protein. This region is followed by a band 4.1-like domain, the common domain in the ezrin, radixin, and moesin family members, which is thought of as a linking segment between the actin cytoskeleton and the cell membrane (Tsukita *et al.*, 1993). The band 4.1-like domain is also present in the product of the neurofibromatosis type 2 tumor suppressor gene, merlin, or schwannomin, and in the *Drosophila melanogaster* tumor suppressor *expanded*, a protein involved in the control of cell proliferation in imaginal discs (Boedigheimer *et al.*, 1993; Tsukita *et al.*, 1993). At its very C-terminal end, PTP-BL harbors the tyrosine phosphatase domain that is catalytically active in vitro on artificial substrates (Hendriks *et al.*, 1995), but in vivo substrates remain to be identified.

In between the band 4.1-like and the PTPase domain, PTP-BL contains five PDZ motifs. PDZ motifs, formerly referred to as GLGF repeats (Cho *et al.*, 1992) or discs-large homologous regions (Woods and Bryant, 1993), were first identified as 90-amino acid (aa) repeats in PSD-95, DlgA, and ZO-1. The *Drosophila* protein DlgA is the prototype of the family of membrane-associated guanylate kinases. These proteins contain one or three N-terminal PDZ motifs, an SH3 motif, and a guanylate kinase motif and are localized to specialized submembranous structures. DlgA is required for the maintenance of the septate junction structure, for the proper organization of the cytoskeleton, and for apicobasal polarity of epithelial cells (Woods *et al.*, 1996). Other members of this rapidly growing protein family were found to interact with the cytoplasmic tail (T/SxV) of Shaker-type K^+ channels and of modulatory subunits (NR2) of NMDA-type glutamate receptors (Kim *et al.*, 1995; Kornau *et al.*, 1995; Niethammer *et al.*, 1996) and thus may play an important role in the clustering of membrane proteins (Garner, 1996; Gomperts, 1996). Recently, the molecular basis of the C-terminal peptide recognition by PDZ motifs was revealed by x-ray crystallography (Doyle *et al.*, 1996). It appears that specific side chain interactions and a prominent hydrophobic pocket at the PDZ motif surface explain the selective recognition of the last four or five C-terminal residues of the target protein. The binding to C-terminal peptide motifs is mediated by an antiparallel interaction between β-strands and is reminiscent of the manner in which PID/PTB domains associate with phosphotyrosine-containing peptides (Doyle *et al.*, 1996). In addition, it appears that PDZ motifs do not recognize exclusively carboxyl-terminal motifs. For example, the binding of the PDZ motif in INAD to the TRP Ca^{2+} channel is critically dependent on an interaction with an internal STV peptide (Shieh and Zhu, 1996). Furthermore, work on neuronal nitric oxide synthase (nNOS) suggests that specific PDZ motifs can recognize carboxyl-terminal peptide motifs as well as forming apparently homophilic associations with other PDZ motifs (Brenman *et al.*, 1996; Schepens *et al.*, 1997; Stricker *et al.*, 1997). Most recently, a PDZ motif in actinin-associated Lin-11, Isl-1, Mec-2 (LIM) protein has been described that binds to the spectrin-like motifs of α-actinin-2 (Xia *et al.*, 1997).

Our search for proteins that bind to the five PDZ motifs present in PTP-BL now provides evidence for yet another type of interaction that can be mediated by PDZ motifs. The second PDZ motif of PTP-BL as well as the PDZ motif of RIL (reversion-induced LIM gene; Kiess *et al.*, 1995) itself were found to bind specifically to the RIL-LIM domain structure. The fourth PDZ motif of PTP-BL can also interact with RIL, but for this interaction to occur both the LIM domain and the proper carboxyl terminus of RIL are necessary. Thus, along with PDZ-C terminus and PDZ internal peptides, PDZ-LIM interactions may also contribute to the complex organization and dynamics of macromolecular assemblies at the cell cortex.

MATERIALS AND METHODS

Interaction Trap Assay

Plasmid DNAs and the yeast strain used for the interaction trap assay were provided by Dr. Roger Brent and colleagues (Massachusetts General Hospital, Boston, MA) and used as described (Gyuris *et al.*, 1993). From 10^6 transformants of a human G0-fibroblast library (a kind gift from Dr. C. Sardet, Cambridge, MA), 12 clones were retrieved showing an interaction. Comparison of cDNA sequences with database entries were done using the BLAST program (Altschul *et al.*, 1990). Two of the clones were found to represent overlapping RIL cDNAs. The sequence content and schematic representation of the various PTP-BL and RIL peptide regions used in the two-hybrid interaction trap are shown in Figure 1. The single PTP-BL PDZ motifs were obtained by polymerase chain reaction (PCR) using specific primers with PTP-BL cDNA (European Molecular Biology Laboratory [EMBL] accession number Z32740, Hendriks *et al.*, 1995) as a template, and cloned in-frame in the pEG202 bait vector (Gyuris *et al.*, 1993) using standard procedures. The band 4.1-like, PDZ-(I–V), and PTPase domain of PTP-BL and the PDZ motif of RIL were introduced in the pEG202 vector by standard subcloning procedures. The deletion constructs of RIL (Figure 7) were made by subcloning the appropriate restriction fragments [full-length mouse RIL (mRIL-FL), mRIL(209–330), mRIL(209–309), mRIL(249–309), mRIL(249–330), and mRIL(309–330)] or specific PCR fragments [mRIL(315–330), mRIL(209–326), and mRIL(TIVGIQ)] of mouse RIL in-frame in the pJG4–5 prey vector (Gyuris *et al.*, 1993). All constructs generated by PCR were checked for muta-

tions by DNA sequencing. For two-hybrid interaction assays, plasmids were introduced in yeast strain EGY48 and tested for an interaction on minimal agar plates lacking histidine, tryptophan, uracil, and leucine, containing 2% galactose, 1% raffinose, and 80 μg/ml of 5-bromo-4-chloro-3-indolyl-β-D-galactopyranoside (X-gal).

β-Galactosidase Activity Assay

Determination of the relative strength of two-hybrid interactions was done by measuring the β-galactosidase activity in crude yeast lysates. A single yeast colony was inoculated in 1.5 ml of minimum medium lacking histidine, Trp, and uracil containing 2% galactose and 1% raffinose and grown overnight until $OD_{600nm} \approx 1.0$. Cells were pelleted and resuspended in 0.2 ml of ice-cold buffer (0.1 M NaCl, 10 mM Tris-HCl, pH 7.0, 1 mM EDTA, 1 mM phenylmethylsulfonyl fluoride). About 100 μl of acid-washed glass beads (425–600 μm, Sigma Chemical, St. Louis, MO) were added, and the suspension was vortexed six times for 30 s, alternated with 30-s incubations on ice. Lysates were centrifuged for 5 min with 14,000 rpm at 4°C. Supernatants were transferred to fresh tubes and used for protein concentration determination (Bradford, 1976). β-Galactosidase activity was measured by adding 10 μl of lysate to 200 μl of freshly prepared ONPG buffer (100 mM phosphate buffer, pH 7.0, 1 mM MgCl, 10 mM KCl, 50 mM β-mercaptoethanol, 0.35 mg/ml *O*-nitrophenyl-β-D-galactopyranoside, Sigma) in microtiter plates. Reactions were incubated at 30°C and the OD_{420nm} was monitored for 1 h on a CERES UV900C MTP-photometer (Bio-Tek, Winooski, VT). The specific β-galactosidase activity (arbitrary units) was calculated using the initial linear part of the OD_{420nm}/min curves and corrected for the protein concentration of the sample.

Isolation and Sequencing of Mouse RIL cDNAs

The 0.6-kb pair hRIL(164–330) insert, encoding the C terminus of human RIL (hRIL), was isolated, labeled radioactively by random priming, and used to screen a mouse brain λ-ZAPII cDNA-phage library (Stratagene, La Jolla, CA) following standard procedures. Of 0.65×10^6 plaques, two were found to be positive for the RIL cDNA. These phages were plaque purified and inserts were rescued as pBluescript SK^- plasmids according to the manufacturer's protocols. Nucleotide sequences were determined by double-stranded DNA dideoxy sequencing using T3 and T7 sequencing primers on rescued plasmids and derived subclones. The mRIL-FL–cDNA sequence was compared with database entries using the BLAST program (Altschul *et al.*, 1990). Alignments with RIL cDNAs from various species and other PDZ-containing proteins were made using MULTALIGN, were adapted manually, and homologies were calculated using DISTANCES (Program Manual for Wisconsin Package, Version 8, Genetics Computer Group, Madison, WI).

Polyclonal Antibodies (pAbs)

Restriction fragments encoding aas (amino acids) 1056–1284 (including PDZ-I) or aas 2101–2460 (including the PTPase domain) of PTP-BL and the insert of hRIL(164–330; encoding the C-terminal half of hRIL) were cloned in appropriate pGEX prokaryotic expression vectors (Pharmacia, Piscataway, NJ). GST-fusion proteins were isolated (Frangioni and Neel, 1993) and used to immunize rabbits. Affinity-purified pAbs (α-BL-PDZ-I, α-BL-PTP, and α-RIL, respectively) were obtained by applying whole serum to Affigel-15-immobilized (Bio-Rad, Richmond, CA) purified GST-fusion protein and eluting bound antibodies.

Transient Expression and Immunoprecipitation

Mouse PTP-BL and RIL protein parts were expressed from the eukaryotic expression vector pSG5 (Green *et al.*, 1988), which was modified to generate an in-frame VSV epitope tag for detection or immunoprecipitation of the produced peptide using the monoclonal anti-VSV antibody P5D4 and, if necessary, an initiator AUG codon or a stop codon. hRIL(164–330) was expressed from the eukaryotic expression vector pMT.HAtag, a modified pMT2 vector that contains an initiator AUG codon followed by a hemagglutinin epitope tag sequence immediately upstream of the cloning site (Serra Pages *et al.*, 1995), and mRIL-FL was expressed from the pSG5 expression vector by cloning the mRIL-FL-3 cDNA, containing its own initiator AUG codon, in the multiple cloning site. COS-1 cells were cultured in DMEM/10% fetal calf serum. For each assay, 1.5×10^6 cells were electroporated at 0.3 kV and 125 μF using the Bio-Rad GenePulser with a 4-mm electroporation cuvette, in 200 μl of phosphate-buffered saline (PBS) containing 10 μg of plasmid DNA. Cells were plated on a 10-cm dish and cultured for 48 h in DMEM/10% fetal calf serum. Cells were harvested by scraping in ice-cold PBS, pelleted by centrifugation (1000, 5 min), and lysed in 500 μl of lysis buffer (50 mM Tris-HCl, pH 8.0, 150 mM NaCl, 5 mM EDTA, 0.5% Non-Idet P-40, 1 mM phenylmethylsulfonyl fluoride, 10 μg/ml aprotinin, 10 μg/ml leupeptin, 10 μg/ml pepstatin A). After a 1-h incubation on ice, the lysate was centrifuged for 10 min at $10{,}000 \times g$ at 4°C and the supernatant was cleared with 20 μl of protein A-Sepharose CL-4B (Pharmacia) for 2 h rotating at 4°C. After addition of monoclonal antibody (mAb) P5D4 (2 μl of ascites fluid) or pAb α-RIL (5 μg affinity purified) and rotation for 2 h at 4°C, 30 μl of protein A-Sepharose CL-4B were added and incubation was prolonged overnight. The immunoprecipitates were washed four times with 0.5 ml of lysis buffer and boiled for 5 min in 20 μl of 2× sample buffer (100 mM Tris-HCl, pH 6.8, 200 mM dithiothreitol, 4% SDS, 0.2% bromophenol blue, 20% glycerol), and proteins were resolved on 12% polyacrylamide gels and transferred to nitrocellulose membranes by Western blotting. Blots were blocked using 5% nonfat dry milk in 10 mM Tris-HCl (pH 8.0), 150 mM NaCl, and 0.05% Tween 20 (TBST). Affinity-purified pAb α-RIL (1:1000 dilution) was used to detect coprecipitation of RIL protein and mAb PY-20 (Transduction Laboratories, 1 μg/ml) to detect tyrosine phosphorylated proteins. Incubations with primary and secondary antibodies [alkaline phosphatase-conjugated AffiniPure goat anti-rabbit IgG (0.06 μg/ml), Jackson ImmunoResearch Laboratories, West Grove, PA] and subsequent washes were done in TBST. Labeled bands were visualized using CPD Star chemiluminescence according to the manufacturer (Tropix, Bedford, MA).

Immunofluorescence Assay

Cryosections of unfixed tissues (6 μm) were cut and mounted on Superfrost/Plus slides (Menzel Gläser, Germany). After thawing, sections were fixed for 5 min in cold methanol (−20°C) for α-BL-PDZ-I and α-BL-PTP or in 3% paraformaldehyde in PBS for α-RIL, and subsequently washed twice with PBS/0.05% Tween 20 (PBST). Tissue sections were incubated in affinity-purified pAb (diluted 1:200 in PBST) for 1 h at room temperature in the presence of 1% normal swine serum and washed three times for 5 min in PBST. Specific labeling was detected by subsequent incubation in fluorescein-conjugated swine anti-rabbit IgG (12 μg/ml, Dako, Carpinteria, CA) in PBST for 1 h and washing in PBST. Sections were mounted in Mowiol (Sigma). Hematoxylin/eosin-stained sections were prepared according to standard histological procedures.

In Vitro Tyrosine Phosphorylation and Dephosphorylation Assay

The plasmid encoding GST-BL-PTP (aas 2101–2460) was generated as described above. GST-RIL-PDZ (aas 1–101) and GST-RIL-LIM (aas 209–330) were made by subcloning restriction fragments of mRIL-FL in the appropriate pGEX vector. The tyrosine-to-phenylalanine mutant of the RIL-LIM domain, GST-RIL-LIM-Y-F (aas 209–330), was made by PCR using oligonucleotides harboring the desired mutation and GST-RIL-LIM as a template. The mutated sequence of GST-RIL-LIM-Y-F was confirmed by sequencing. GST-fusion proteins were produced in bacterial TKX cells according to

the supplier's instructions (Stratagene). Cells were lysed by sonification in PBS containing protease inhibitors (1 mM phenylmethylsulfonyl fluoride, 10 μg/ml aprotinin, 10 μg/ml leupeptin, 10 μg/ml pepstatin A) and GST-fusion proteins were purified using glutathione-Sepharose CL-4B (Pharmacia) and analyzed on 12% polyacrylamide gels. Samples representing about 1 μg of fusion protein were loaded on each lane and the presence of GST-fusion protein and tyrosine phosphorylation was detected by Western blotting using the mAbs 2F3 (α-GST) and PY-20 (α-P-tyr, Transduction Laboratories, Lexington, KY), respectively. For the dephosphorylation assay, 1 μg of purified phosphorylated GST-RIL-LIM was incubated for 15 min at 37°C in PBS containing protease inhibitors with 0.1 μg of purified GST-BL-PTP or, as a control, with 0.1 μg of GST. As a specific protein tyrosine phosphatase inhibitor, $NaVO_3$ was used at a final concentration of 1 mM.

RESULTS

The Reversion-induced LIM-containing Protein RIL Interacts with PTP-BL PDZ Motifs

Candidate proteins interacting with the five PDZ motifs of PTP-BL were obtained from a human G0-fibroblast cDNA library using BL-PDZ-(I–V) (Figure 1A) as a bait in the yeast two-hybrid interaction trap (Gyuris *et al.*, 1993). Sequence analysis showed that two independent but overlapping clones of 0.6 and 0.5 kb pairs encoding the C-terminal part of the human homologue of rat RIL were obtained [Figure 1B, hRIL(164–330) and hRIL(188–330), respectively]. RIL was originally identified as a gene that is down-regulated in H-Ras–transformed rat fibroblasts (Kiess *et al.*, 1995).

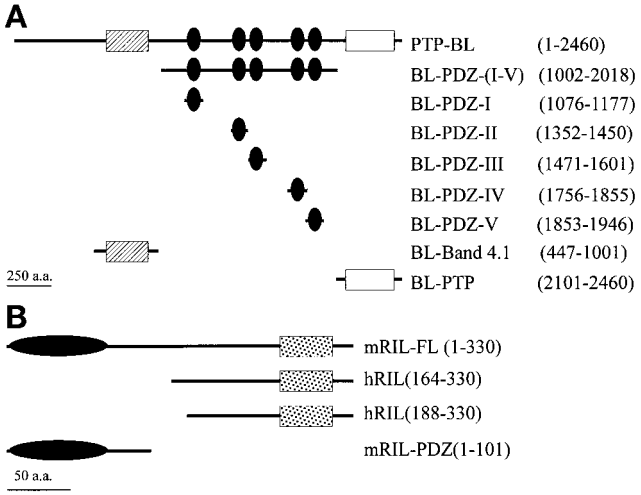

Figure 1. Schematic representation of the protein segments used in the two-hybrid interaction trap. Shown are the regions of PTP-BL (A) used as baits and the RIL segments [hRIL(164–330) and hRIL(188–330)] (B) as they were retrieved from the G0-fibroblast cDNA library and the RIL-PDZ domain used as bait to assay for intramolecular interactions. In parentheses, the numbers corresponding to the first and last aa positions in the PTP-BL and RIL segments are shown. Band 4.1-like domain, hatched box; PTPase, open box; PDZ motifs, black ovals; LIM domain, stippled box.

The RIL protein contains a single LIM domain at its C terminus, which is a special double zinc finger motif implicated in protein–protein interactions in a broad range of polypeptides (reviewed by Dawid *et al.*, 1995). The LIM domain is entirely present in our partial hRIL-cDNA clones (Figures 1B and 2). Comparison of the RNA in situ hybridization patterns of RIL (Kiess *et al.*, 1995) and PTP-BL (Hendriks *et al.*, 1995) revealed a conspicuous overlap in expression, implying that the interaction observed may indeed be of biological relevance.

To further study this interaction, a mouse fetal brain cDNA library was screened using the human 0.6-kb pair RIL-cDNA insert as a probe. Two cDNAs of 1.2 and 1.5 kb pairs, respectively, were obtained and their combined sequence (EMBL Nucleotide Sequence Database accession number Y08361) predicts an open reading frame resulting in a 330-aa polypeptide with a predicted molecular weight of 36,000 (Figure 2). Transient expression of the cDNAs employing the pSG5 vector (Green, 1988) in COS-1 cells resulted in a protein product with an apparent molecular weight of 38,000. This is identical in size to endogenous RIL as detected on Western blots of several mouse tissue

```
                10         20         30         40         50
mouse MTHSVTLRGP SPWGFRLVGG RDFSLPLTIS RVHAGSKAAL AALCPGDLIQ
rat   ---A------ ---------- ----A----- ---------- -------S--
human -P-------- ---------  ----A----- --------S- ----------

                60         70         80         90        100
mouse AINGESTELM THLEAQNRIK GCHDHLTLSV SRPENKNWPS SPDD KAQAHR
rat   ---------- ---------- ---------- ---------- --N- ------
human ---------- ---------- ---------- ----GRS--- A---S------

               110        120        130        140        150
mouse IHIDPEFQDC SPATSRRSSV SGISLEDNRS GLGSPYGQPP RLPVPHNGSS
rat   ------A--G ---------I ---------- ---------- ----------
human ------I--G -T-----P-G T-TGP--G-R S------K-- CF--------

               160      ↓ 170        180          ↓ 200
mouse NEATLPAQMS ALHVSPPTSA DTARVLPRNR DCRVDLGSEV YRMLREPAEP
rat   --V---S--- -------P-- --P-I----- ---------- ----------
human  --------- -------P-- -P-EA S-GA GS-------- ----------

               210        220        230        240        250
mouse TASEPKQSGS FRYLQGMLEA GEGGDRPGSG GPRNLKPAAS KLGAPLSGLQ
rat   A--------- ---------- ---------- -S-------- ----------
human V-A------- ---------- -----W--P-- -------T-- ----------

               260        270        280        290        300
mouse GLPECTRCGH GIVGTIVKAR DKLYHPECFM CSDCGLNLKQ RGYFFLDERL
rat   ---------- ---------- ---------- ---------- ----------
human --------C- --------E- ---------- ---------- ----------

               310        320        330
mouse YCENHAKARV KPPEGYDVVA VYPNAKVELV *
rat   ---------- ---------- ----------
human --S------- ---------- ----------
```

Figure 2. Sequence alignment of RIL protein sequences from mouse, rat, and human. Protein sequences of mouse (accession number Y08361), rat (Kiess *et al.*, 1995; accession number X76454), and hRIL (Schaefer, unpublished data; accession number X93510) were aligned using MULTALIGN. aas identical to those of the mouse sequence are indicated with a dash. The PDZ motif is double underlined and the LIM domain is indicated by a single underline. Vertical arrows indicate the start positions of clones hRIL(164–330) and hRIL(188–330), which were originally identified in the two-hybrid interaction screening with the BL-PDZ-(I–V) bait. A potential tyrosine phosphorylation site is shaded.

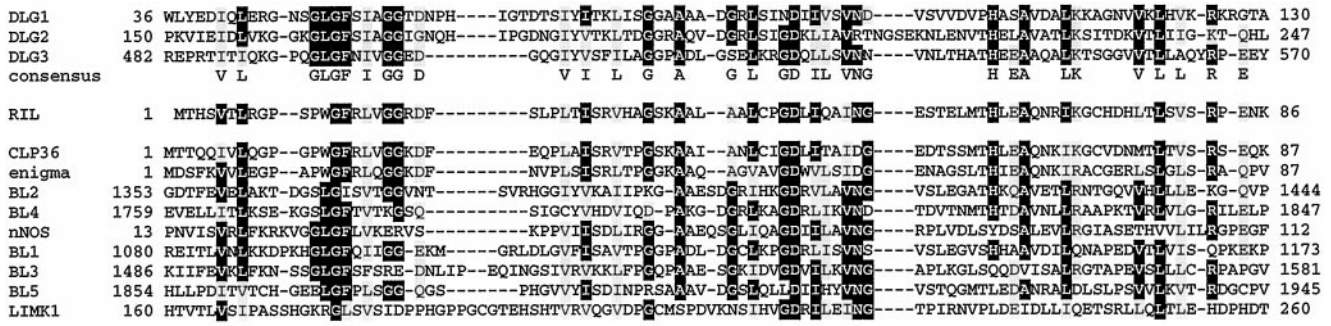

Figure 3. Multiple alignment of PDZ motifs. The PDZ motif of mouse RIL is aligned with the PDZ motifs of *Drosophila* DlgA (DLG1, DLG2, and DLG3; accession number M73529), mouse PTP-BL (BL1 through BL5; accession number Z32740), rat CLP36 (accession number U23769), human enigma (PIR:A55050), mouse nNOS (accession number D14552), and mouse LIMK1 (accession number X86569). The position number of the initial and last aa of the protein segments that were used are shown on either side of the sequence. Sequences presented below RIL are ordered by descending homology. Aas similar (score >0.7 in Dayhoff table; Schwartz and Dayhoff, 1979) in 9 of 13 sequences are shown on a gray background, and the most frequent aa at these positions is indicated in the consensus line. Aas identical in more than half of the sequences are indicated in white on a black background. Dashes represent sequence gaps.

lysates by an affinity-purified polyclonal antiserum raised against the C-terminal half of hRIL (our unpublished results).

Comparison of mouse, human, and rat RIL sequences revealed a high species conservation (Figure 2). The mouse peptide is 96% identical to rat RIL and 87% identical to hRIL. Highest homologies were found at the N and C termini, suggesting a biological relevance for these regions. The C-terminal end brackets the LIM domain (aas 253–303), but in the N terminus initially no conserved protein motif was discerned. Surprisingly, by performing more detailed database searches, we found that the N-terminal segment showed significant similarities to proteins known to contain PDZ motifs. This led to the identification of a previously undiscovered N-terminal PDZ motif (aas 4–84) in RIL (Figure 3) that shows 40–45% homology to any of the three PDZ motifs of DlgA. It is most homologous to thus far unnoticed N-terminal PDZ motifs in CLP-36 (77%; Wang *et al.*, 1995) and enigma (67%; Wu and Gill, 1994). In the 150-aa spacer region between the PDZ motif and the LIM domain of RIL, the identity between species is much lower and no protein motifs could be identified. Interestingly, a potential tyrosine phosphorylation site ([RK]-x(2,3)-[DE]-x(2,3)-Y) was found within the LIM domain (Y-274).

Both the Second and Fourth PTP-BL PDZ Motif Can Interact with RIL

To narrow down the areas involved in the PTP-BL–RIL interaction, single BL-PDZ motifs were fused to the LexA bait (Figure 1A) and assayed for an interaction with both the partial hRIL clone [hRIL(164–330)] and mRIL-FL in the yeast two-hybrid interaction trap (Figure 4). None of the baits used was able to activate transcription without prey (our unpublished results) or with an empty prey vector present (Figure 4). For an interaction with hRIL(164–330) and mRIL-FL to occur, the presence of the second (aas 1352–1450) or the fourth (aas 1756–1855) PDZ motif of PTP-BL was both necessary and sufficient. Furthermore, no interaction could be observed between RIL and the band 4.1-like domain or the PTPase domain of PTP-BL (Figure 4). This does not necessarily imply, however, that RIL is not a substrate for PTP-BL. Tyrosine phosphorylation levels are extremely low in yeast, and proper

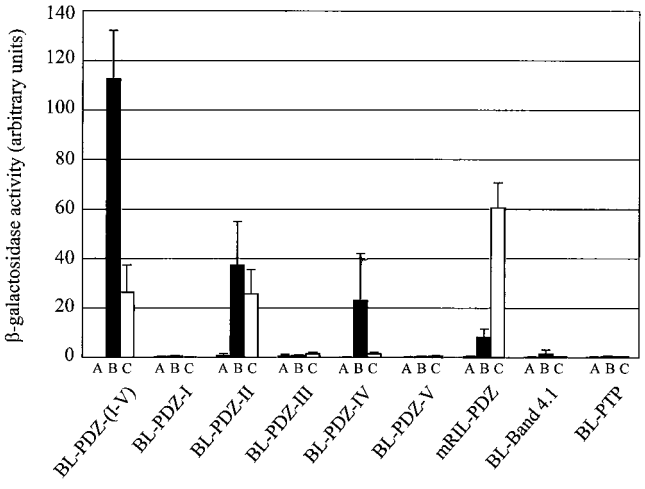

Figure 4. Determination of the relative strength of two-hybrid interactions. β-Galactosidase activities (arbitrary units) were measured in total lysates of yeast containing an LacZ-reporter plasmid. The yeast cells contained plasmids encoding baits as indicated below the bars, and the empty prey vector pJG4–5 (A, gray bars), hRIL(164–330 (B, filled bars), or mRIL-FL (C, open bars). Error bars indicate SD (n = 5).

Table 1. Two-hybrid interaction trap assays to test for PDZ–PDZ and LIM–LIM interactions

	BL-PDZ-(I-V)	RIL-PDZ	mRIL(209-330)
BL-PDZ-(I-V)	−	−	+
RIL-PDZ	−	−	+
mRIL(209-330)	+	+	−

Baits (top row) and preys (vertical row) were constructed and used as described in MATERIALS AND METHODS. +, interaction (blue colonies after 3 d); −, no interaction (no blue colonies after 7 d).

phosphorylation of RIL may be a necessary prerequisite for such an interaction.

Interestingly, the interaction appears weaker if a single PDZ motif is used as a bait, compared with the bait containing the five PDZ motifs [BL-PDZ-(I–V)]. This difference may be explained by the ability of BL-PDZ-(I–V) bait to bind more than one prey protein, leading to stronger transcription activation of the reporter and thereby to a higher β-galactosidase activity in this assay. Another explanation may be that the second and fourth PTP-BL PDZ motifs bind in a cooperative way to one RIL molecule, thereby stabilizing the interaction. Finally, BL-PDZ-(I–V) may form large aggregates through PDZ–PDZ interactions and recruit multiple, synergistically acting prey proteins to the complex. Therefore, we tested whether the PDZ motifs of PTP-BL and RIL can mediate homotypic interactions. Because no evidence was found for this type of interaction (Table 1), we may exclude the latter model as an explanation for our observations.

Furthermore, our results indicate that in contrast to BL-PDZ-II, the interactions of BL-PDZ-(I–V) and BL-PDZ-IV with the mRIL-FL are significantly weaker than with the partial hRIL (Figure 4). This effect is not caused by differences between mouse and hRIL sequences, because similar results were obtained with the partial mouse RIL clone [mRIL(209–330)] (Figure 7). These data suggest the presence of a negatively regulating element located in the N-terminal part of RIL, which does not affect BL-PDZ-II binding.

RIL Can Be Coprecipitated with BL-PDZ Motifs

Although the two-hybrid interaction trap is a very powerful tool to identify potential partner proteins, interactions need to be confirmed in test systems that can provide the normal cellular environment of the molecules involved. Therefore, we have transiently coexpressed epitope-tagged PDZ motifs and RIL in mammalian epithelial cells (COS-1) as substrates for immunoprecipitation. Pull-down of the product of the partial RIL cDNA [hRIL(164–330)] was demonstrated for BL-PDZ-(I–V), BL-PDZ-II, and BL-PDZ-IV (Figure 5), confirming the results obtained in the yeast two-hybrid interaction trap. Again, no interaction between the band 4.1-like and the PTPase domain of PTP-BL with RIL was observed. Strikingly, coprecipitation with single PDZ motifs (BL-PDZ-II and BL-PDZ-IV) is much less efficient than with BL-PDZ-(I–V). This is not a concentration effect because the amount of epitope-tagged PDZ motif present in the extracts, as determined by Western blotting, was comparable for all constructs used (our unpublished observations). The difference in the amount of coprecipitated RIL is significantly more than twofold, excluding binding by BL-PDZ-(I–V) of two RIL molecules (via PDZ-II and PDZ-IV) as the only explanation for this phenomenon. Interestingly, we consistently observed very low concentration of RIL-FL in our lysates (Figure 8). This probably explains why coprecipitation of RIL-FL was barely detectable (our unpublished results). Preliminary observations indicate a rapid degradation of RIL-FL (our unpublished observations), which in vivo may be an important regulatory element in RIL function.

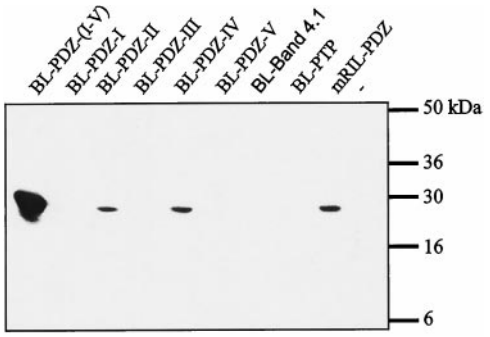

Figure 5. Coprecipitation of RIL with PDZ motifs. VSV epitope-tagged PDZ motifs of PTP-BL and RIL were transiently coexpressed in COS-1 cells with the C-terminal part of RIL, hRIL(164–330). α-VSV mAbs were used to immunoprecipitate the various PDZ proteins. Coprecipitated RIL was detected by Western blotting using a pAb (α-RIL) directed against the C-terminal part of hRIL. The labels on top refer to the protein segments outlined in Figure 1 and the dash indicates mock-transfected cells.

PTP-BL and RIL Colocalize In Situ

To substantiate the possible biological relevance of the PTP-BL–RIL interaction, we studied the tissue distribution and subcellular localization of these proteins by immunohistological assays (Figure 6). Affinity-pu-

Figure 6 (facing page). Colocalization of PTP-BL and RIL in mouse tissues. Visualization of the presence of PTP-BL and RIL proteins in mouse lung, stomach, and skin was done using immunofluorescence labeling with affinity-purified polyclonal antiserum directed against PTP-BL (α-BL-PDZ-I and α-BL-PTP) and RIL (α-RIL). Corresponding hematoxylin/eosin-stained sections (HE) are shown for comparison. Bars, 25 μm.

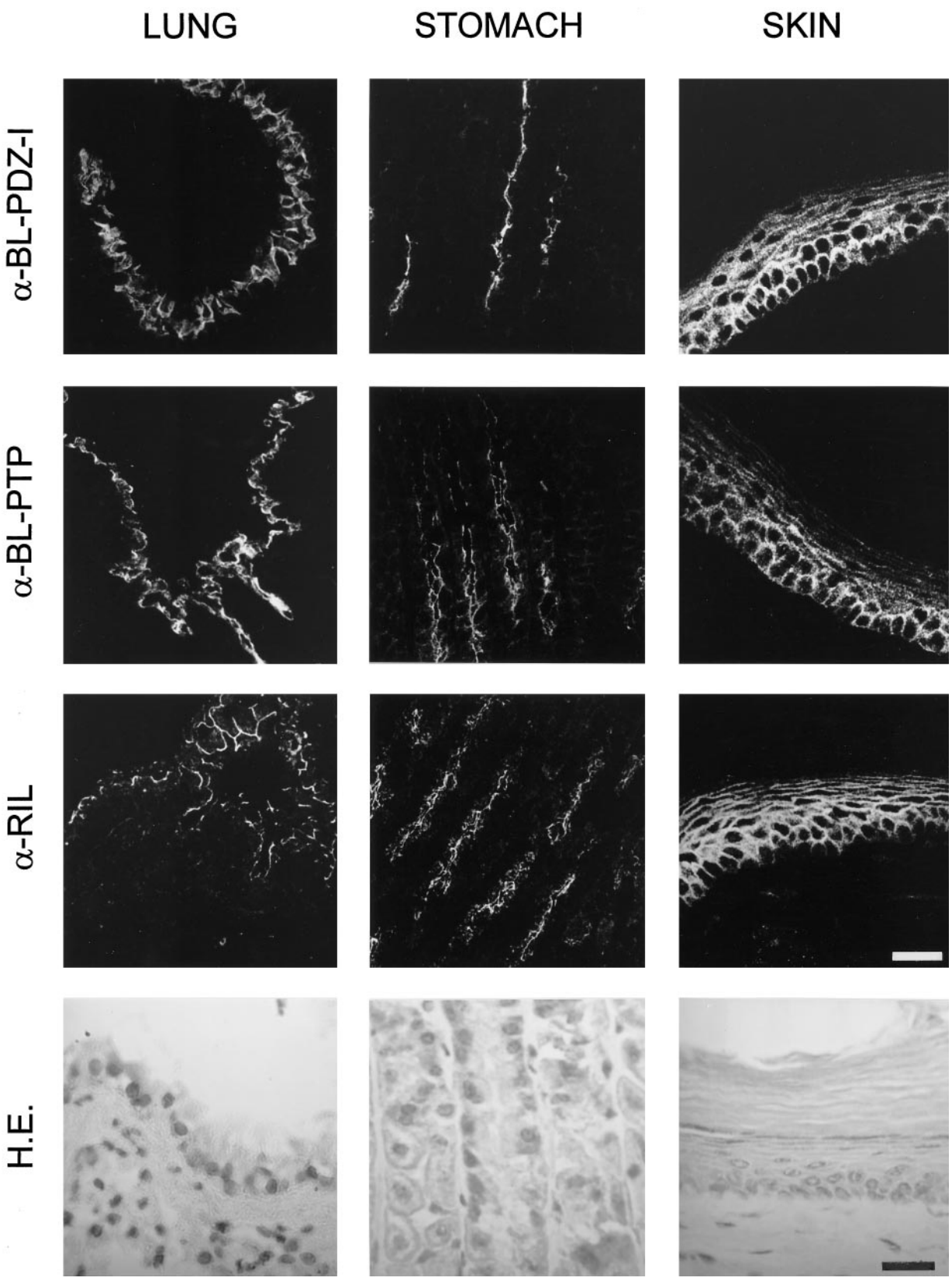

Figure 6.

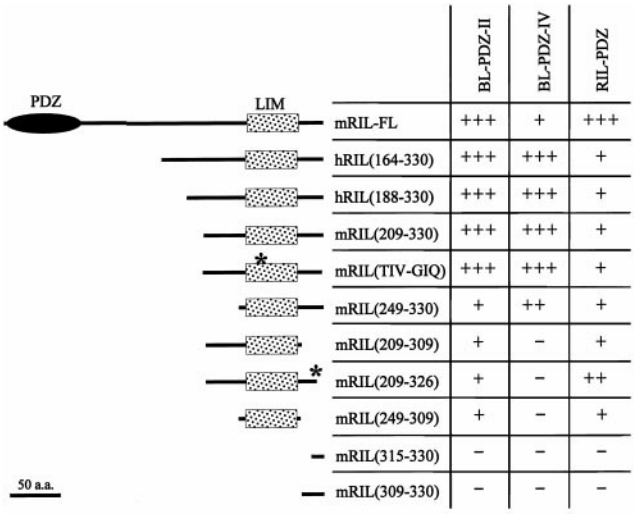

Figure 7. PDZ-mediated interactions with truncated RIL peptides. Schematic representation of the regions of RIL used as prey in the two-hybrid interaction trap are shown on the left. Interaction results using these constructs combined with BL-PDZ-II, BL-PDZ-IV, and mRIL-PDZ as baits are represented by + and −. +++, very strong interaction (blue colonies within 2 d on X-gal assay plates); ++, interaction (blue colonies after 3 d); +, weak but detectable interaction (blue colonies after 4–6 d); −, no interaction detectable (no blue colonies after 7 d).

rified rabbit polyclonal antiserum against PTP-BL (α-BL-PDZ-I and α-BL-PTP) and hRIL (α-RIL) were used to detect the endogenous proteins. The results are in full agreement with those obtained by previous RNA in situ hybridization studies (Hendriks *et al.*, 1995; Kiess *et al.*, 1995). Expression of both proteins could be observed in various mouse epithelia. Detailed examination of lung cryosections revealed that the epithelium covering the bronchi expresses high amounts of both PTP-BL and RIL, whereas other parts of the lung show no detectable expression. PTP-BL and RIL are both expressed exclusively at the apical site of these epithelial cells. High expression levels were also found in the glandular part of the stomach, and again both RIL and PTP-BL are consistently detected apically in all epithelial cell types studied. In corneal epithelium of mouse skin and in the nonglandular part of the stomach (our unpublished observations), both proteins are distributed in dot-like structures close to the cellular membrane, suggestive of a desmosome-like pattern. In fact, all near-membrane regions in the epidermis are positive for both PTP-BL and RIL except for the basement membrane of the basal cell layer, which is negative for both proteins. The dermis and stratum corneum were found to be completely negative, whereas epithelia covering glands and hair follicles were again positive (our unpublished observations). Taken together, we may conclude that PTP-BL and RIL are coexpressed apically in all polarized epithelial cell types studied so far, where they may play a role in the establishment or maintenance of the polarized phenotype of these cells.

The RIL-LIM Domain Is Necessary for Interaction with PTP-BL PDZ Motifs

Having shown the possibility for PTP-BL and RIL to interact in vivo, we next studied the molecular basis of their association. To determine the minimal region in RIL necessary for an interaction with the PTP-BL PDZ motifs, a series of N- and C-terminally truncated RIL peptides was used as a prey in the interaction trap along with BL-PDZ-II and BL-PDZ-IV as baits (Figure 7). For BL-PDZ-II the entire RIL-LIM-domain, including flanking N- and C-terminal sequences, is needed to enable a strong interaction. Further truncation toward the LIM domain resulted in a weaker but still significant interaction (as determined by β-galactosidase activity measurements of total yeast lysates; our unpublished results). It is important to note that deletion of the last four RIL residues [mRIL(209–326)] does not affect binding. This defines the minimal region of RIL necessary for interaction with BL-PDZ-II to the polypeptide stretch between aa positions 249 and 309, which is essentially the complete LIM domain (Figure 7).

In the same way, the minimal region of RIL for BL-PDZ-IV interaction was determined and assigned to the complete segment between aas 249 and 330 (Figure 7). In contrast to BL-PDZ-II, deletion of the C-terminal 21 residues or the last 4 residues of RIL resulted in the abolishment of any detectable interaction, indicating that these residues are most relevant for interaction with BL-PDZ-IV. However, the C-terminal 15 or 21 residues alone, which are 100% conserved between mouse and human, did not show any interaction (Figure 7). These results indicate that both the LIM domain and the proper C terminus are necessary for a strong BL-PDZ-IV interaction with RIL, clearly distinguishing this mode of interaction from that described for PDZ motifs with C-terminal peptides (Doyle *et al.*, 1996) and also from the interaction between BL-PDZ-II and the RIL-LIM domain reported here.

Because C-terminal consensus-binding sequences have been determined for PDZ-II and IV of PTP-BAS by screenings of oriented peptide libraries (Songyang *et al.*, 1997), we looked for the presence of these motifs in the entire RIL molecule. The last four residues of RIL are −VELV and the consensus for PDZ-II and IV binding are −(E/V)(T/S)X(V/I) and −(I/Y/V)YYV, respectively, which should be considered a very weak match. Strikingly, there is an internal TIV motif within the first loop of the LIM domain. However, mutation of this TIV to GIQ did not affect the BL-PDZ-II or -IV interaction with RIL (Figure 7). This contrasts mark-

edly with the INAD PDZ motif-binding characteristics to the 19-aa C terminus of TRP, which contains an essential internal (S/T)XV motif (Shieh and Zhu, 1996).

The RIL-LIM Domain Is Phosphorylated on Tyrosines In Vitro and In Vivo and Is an In Vitro Substrate for PTP-BL

Our results clearly indicate that the entire RIL-LIM domain is necessary for the interaction with PTP-BL. This domain harbors a potential tyrosine phosphorylation site at position 274. To study whether the RIL-LIM domain can be phosphorylated on tyrosines in vitro and may function as a substrate for PTP-BL, we induced GST-fusion proteins in TKX bacterial cells, which contain an inducible tyrosine kinase (Stratagene). No tyrosine phosphorylation of GST alone or GST-PDZ could be detected by Western blot analysis, whereas GST-RIL-LIM was phosphorylated on tyrosines in this bacterial system (Figure 8A). The bands of lower molecular weight in the GST-RIL-LIM lane are most probably due to degradation of the fusion protein. Although there are several tyrosines within the GST-RIL-LIM sequence, only tyrosine 274 was predicted to be a substrate for tyrosine kinases by the PROSITE database. Therefore, we mutated this tyrosine to a phenylalanine (GST-RIL-LIM-Y-F). The tyrosine phosphorylation of the Y274F mutant fusion protein is markedly reduced (Figure 8A), but other tyrosine residues are phosphorylated as well in this bacterial system.

The fact that tyrosine-phosphorylated GST-RIL-LIM can be dephosphorylated by addition of purified GST-BL-PTP, whereas GST alone had no effect (Figure 8B), clearly demonstrates that the phosphorylated RIL-LIM domain is an in vitro substrate for PTP-BL. Moreover, the specific tyrosine phosphatase inhibitor vanadate can completely inhibit the tyrosine dephosphorylation by GST-BL-PTP (Figure 8B).

To study this phosphorylation in a more physiological context, we immunoprecipitated the RIL-LIM domain hRIL(164–330) and mRIL-FL from transiently overexpressing COS-1 cells that were treated for 15 min with vanadate. The presence of the RIL protein in the lysate and the immunoprecipitation was demonstrated by Western blotting and immunodetection using α-RIL antibodies (Figure 8C). Tyrosine phosphorylation of both RIL-FL and the RIL-LIM domain was demonstrated by incubating the Western blot with the phosphotyrosine-specific antibody PY-20 (Figure 8D).

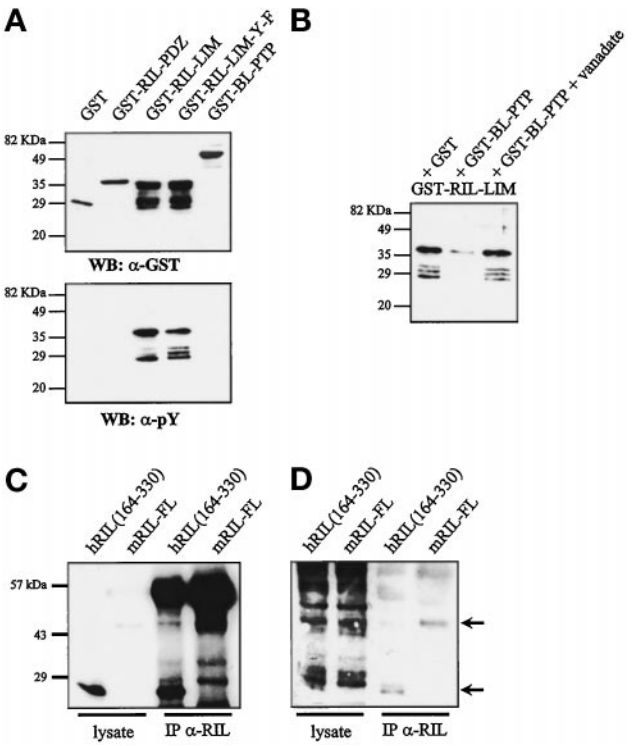

Figure 8. RIL is phosphorylated on tyrosines in vitro and in vivo and is an in vitro substrate for PTP-BL. (A) GST-fusion proteins were purified from bacterial TKX cells expressing an inducible tyrosine kinase. Purified protein was detected by Western blotting using an anti-GST antibody (top panel) and analyzed for tyrosine phosphorylation using the phosphotyrosine specific antibody PY20 (bottom panel). Only GST-RIL-LIM (aas 209–330) is phosphorylated on tyrosines and mutation of tyrosine 294 to phenylalanine (GST-RIL-LIM-Y-F) clearly diminishes the phosphorylation level. (B) Purified phosphorylated GST-RIL-LIM was incubated for 15 min with purified GST or GST-BL-PTP (aas 2101–2460) and analyzed for its phosphotyrosine content. GST-BL-PTP can dephosphorylate the RIL-LIM domain, whereas GST alone does not affect the tyrosine phosphorylation. Furthermore, the specific tyrosine phosphatase inhibitor vanadate can completely inhibit the dephosphorylation by GST-BL-PTP. (C) COS-1 cells were transfected with an expression construct encoding the C-terminal half of RIL [hRIL(164–330)] or mRIL-FL. The presence of transiently expressed RIL in total cell lysates and anti-RIL immunoprecipitates was detected by Western blotting using an anti-RIL antibody. (D) The tyrosine phosphorylation content of the same samples as depicted in C was determined by Western blotting using the phosphotyrosine-specific antibody PY20. Both the immunoprecipitated hRIL(164–330) and the mRIL-FL are found to be phosphorylated on tyrosine residues.

An Intramolecular RIL-PDZ–LIM Interaction

Because RIL contains a PDZ motif itself (Figures 2 and 3), the possibility of an intramolecular interaction between this N-terminal PDZ motif (aas 4–84) and the RIL C terminus was studied. We tested aas 1–101 of RIL (mRIL-PDZ, Figure 1B), containing the entire RIL-PDZ motif, for binding to mRIL-FL or the C-terminal part of RIL [hRIL(164–330)] using the two-hybrid interaction trap. Indeed, a significant interaction was observed, but in contrast to the findings with BL-PDZ-IV, the interaction is much stronger with the RIL-FL than with the truncated protein (Figure 4). This may be explained by the possibility of RIL-FL to form linear multimers via PDZ-LIM interactions, recruiting

multiple prey activation domains to one bait. The possibility of sequence differences between human and mouse RIL influencing the interaction was excluded using truncated mouse RIL [mRIL(209–330)] along with the mouse RIL-PDZ motif, which gave the same results (Figure 7). The testing of truncated C-terminal RIL peptides for their ability to interact with the RIL-PDZ motif demonstrated weak but significant interactions for all constructs containing the LIM domain (Figure 7). Interestingly, the RIL-PDZ motif interacts more strongly with the construct lacking the last four residues [mRIL(209–326)] than with mRIL(209–330), perhaps reflecting an inhibitory effect of these residues on RIL-PDZ binding.

Again, the interaction between the RIL-PDZ motif and the LIM domain could be confirmed by coprecipitation of the RIL C terminus with epitope-tagged RIL-PDZ motif from transiently coexpressing COS-1 cells (Figure 5).

Because it has been shown that LIM domains can engage in homo- and heterodimerization (Feuerstein *et al.*, 1994), we tested the ability of the RIL C terminus (aas 209–330) containing the LIM domain including flanking sequences, to homodimerize using the two-hybrid interaction trap. No interaction was observed by the use of experimental conditions in which RIL-PDZ or BL-PDZ-(I–V) interactions could be readily detected (Table 1).

DISCUSSION

The protein tyrosine phosphatase PTP-BL contains in addition to its catalytic segment a band 4.1-like domain and five PDZ motifs, features that predict a restricted localization at submembranous or cytoskeletal structures within the cell (Tsukita *et al.*, 1993; Ponting and Phillips, 1995). To obtain experimental evidence for this prediction and identify the individual protein constituents in the subcellular microenvironment, a two-hybrid screen was performed using the segment encompassing the five PDZ motifs of PTP-BL as a bait. An interacting protein was obtained that previously had been identified in rat as RIL, the product of a gene that is down-regulated in H-Ras–transformed fibroblasts (Kiess *et al.*, 1995). The interaction was confirmed by transfection experiments in COS-1 cells. Perhaps more importantly, the possible in vivo relevance of this interaction is firmly corroborated by the extensive overlap in RNA expression patterns in mice (Hendriks *et al.*, 1995; Kiess *et al.*, 1995). Also, the fact that both proteins are consistently localized at the same subcellular structures, such as the submembranous apical side of polarized epithelial cells, in mouse tissue sections (Figure 6) supports our view that this interaction must have biological significance. Because PTP-BL is up-regulated by differentiation stimuli in mouse erythroleukemia and embryonal carcinoma (F9) cells (Chida *et al.*, 1995) and RIL is down-regulated in transformed cells (Kiess *et al.*, 1995), it is tempting to speculate that the formation of PTP-BL-RIL complexes is a crucial aspect in the control of growth and differentiation of epithelial cells.

What could be the features that govern binding interaction and determination of PTP-BL-RIL location? The RIL protein contains a C-terminal LIM domain and, in addition, we identified an N-terminal PDZ motif (Figure 3). We demonstrate that these motifs can mediate intermolecular and perhaps intramolecular associations because, like the second and fourth PTP-BL PDZ motif, the RIL-PDZ motif can engage in binding to the RIL-LIM domain (Figures 4, 5, and 7). In view of results obtained in other studies (Kim *et al.*, 1995; Kornau *et al.*, 1995; Niethammer *et al.*, 1996; Songyang *et al.*, 1997), it is striking that ablation of the last four residues of RIL did not affect PDZ-II interaction and enhanced RIL-PDZ binding, whereas no PDZ-mediated interactions could be observed with the RIL C terminus alone (Figure 7). In contrast, for the BL-PDZ-IV binding there is dependence on the integrity of the C terminus of RIL, but again not uniquely on the presence of the very last aa residues only. Random mutagenesis of the RIL-LIM domain confirms the above observations (our unpublished observations).

How can we reconcile these findings to the known properties of PDZ motifs? Thus far, one interaction mode for PDZ motifs has dominated the literature: recognition of a very short carboxyl-terminal sequence motif (Fanning and Anderson, 1996; Gomperts, 1996). The x-ray crystallographic structure of the third PDZ motif from the synaptic density protein PSD-95/SAP90 in the absence and presence of a binding peptide has recently been determined (Doyle *et al.*, 1996) and provides a solid basis for our understanding of the recognition of the T/sxv carboxyl terminus as present in multiple channel and receptor subunits. That PDZ motifs are also able to bind to internal peptide segments has been inferred from studies on the PSD-95/SAP90 interaction with nNOS (Brenman *et al.*, 1996; Schepens *et al.*, 1997). An explanation for this was provided by assuming that not only a C-terminal sequence, but also an internal β-strand may interact with PDZ motifs in a similar manner (Harrison, 1996). This can indeed be witnessed in the crystal structure of the PDZ-III domain of hdlg, which displays a dimer mediated by β-strands in both molecules (Morais Cabral *et al.*, 1996). Also, the binding of the INAD-PDZ motif to the TRP store-operated channel deviates from the carboxyl terminus rule. Although the interaction was localized to the 19-aa C terminus of TRP, it appeared critically dependent on the presence of an internal STV motif (Shieh and Zhu, 1996). It has been proposed that alterations of residues within the carboxylate-binding loop of PDZ motifs

could facilitate this binding of a peptide-internal segment (Fanning and Anderson, 1996). Strikingly, PDZ II and -IV of PTP-BL and also the RIL-PDZ motif share features with INAD, in that they contain an SLGI/F instead of a GLGF motif, and perhaps this represents a signature motif for domains with internal peptide-segment avidity. Further elaborating on an analogy to the INAD PDZ-TRP binding (Shieh and Zhu, 1996), an internal TIV peptide can be found within the first zinc-finger of the RIL-LIM domain. However, mutation of this peptide does not affect the interaction with PTP-BL, indicating that sequences outside this triplet are more important.

Taken together, the experimental data presented here provide compelling evidence for a novel type of protein–protein interaction mediated by PDZ motifs and LIM domain structures that is structurally different from the carboxyl terminus recognition mode by other PDZ motifs. The sequences flanking the LIM domain, including the C terminus, may be directly involved in binding (in the case of PDZ-IV) or they may be important for stabilizing the LIM domain structure. Our results of course do not exclude that the PDZ motifs of PTP-BL can engage in more classical interactions or interactions with proteins other than RIL. For example, screening of an oriented peptide library with PDZ-II of the human homologue of PTP-BL, PTP-BAS, revealed the consensus C-terminal target T/SxV/I (Songyang *et al.*, 1997). This sequence is present in human Fas and indeed it has been shown that PDZ-II of PTP-BL can interact with human Fas (Sato *et al.*, 1996, Cuppen *et al.*, 1997; Saras *et al.*, 1997a) but not with mouse Fas, as this has a different C-terminal end (Cuppen *et al.*, 1997). However, the interaction was found to be 30- to 40-fold weaker than the binding to the RIL-LIM domain in our assays (Cuppen *et al.*, 1997; Figure 4). Also, for nNOS two different binding modes have been described (Schepens *et al.*, 1997), and even the presence of separate binding interfaces on the PDZ protein module cannot be excluded. In fact, a coordinate involvement of different binding interfaces on both the PDZ and the RIL-LIM motifs is suggested by our findings. Coprecipitation of truncated forms of RIL from cell lysates is much more efficient for constructs containing the PTP-BL PDZ motifs II and IV together, than for those harboring a single PDZ motif (Figure 5). This effect cannot just be explained by the binding of two RIL molecules to a single PDZ-(I–V) peptide, and one has to assume a cooperative or stabilizing effect resulting from the binding of two distinct PDZ motifs to one and the same LIM domain. Moreover, the observation that PDZ-II and PDZ-IV differ in their minimal requirements for interaction with RIL-LIM sequences (Figure 7) is in line with the presence of two binding interfaces in the LIM domain. This would explain why the binding of the RIL-PDZ motif to the RIL-LIM domain does attenuate the binding of the fourth but not the second PDZ motif of PTP-BL in the two-hybrid experiments (Figure 4). The possibility of two interacting interfaces on a single LIM domain has also been put forward by Arber and Caroni (1996), and from structural data it can be deduced that distinct binding interfaces may reside in the two independent zinc-finger modules, each with different aa composition of their loop (Hammarstrom *et al.*, 1996; Perez Alvarado *et al.*, 1996).

If the RIL-LIM domain can indeed bind two different PTP-BL molecules, very large clusters could be formed. The unoccupied PDZ motifs of PTP-BL and RIL in this assembly may in turn interact with other proteins, thus generating even larger heterogeneous protein complexes in which the band 4.1-like domain of PTP-BL may be responsible for a proper submembranous localization. The ability of RIL to form an intramolecular PDZ-LIM interaction, inducing disassembly or rearrangements of the complex, could then function as a regulatory principle. It is also conceivable that the phosphorylation of tyrosine residues within the RIL-LIM domain, which we have demonstrated to occur in vitro and in vivo (Figure 8), may function as such a regulatory switch for clustering behavior. In addition, the tyrosine phosphatase domain of PTP-BL may be a determinant of the phosphorylation status of proteins in such a complex. The recent identification of a GTPase-activating protein for Rho, PARG, which can interact with the human homologue of PTP-BL (Saras *et al.*, 1997b) and the colocalization of RIL with F-actin (our unpublished observations), implicate a role for such a multiprotein PTP-BL complex in actin–cytoskeleton dynamics.

The principle of PDZ-LIM–mediated interactions as demonstrated here could have widespread biological significance because, in addition to RIL, several other LIM domain-containing proteins, such as CLP-36, ALP, enigma, LIMK1, and LIMK2 also harbor PDZ motifs intramolecularly (Wu and Gill, 1994; Okano *et al.*, 1995; Wang *et al.*, 1995; Xia *et al.*, 1997). If these proteins function as adapter molecules in bringing together diverse molecules in a defined but dynamic microenvironment at specialized submembranous or cytoskeletal structures, a disturbance of such structures could lead to pathological phenomena like tumorigenesis and developmental abnormalities. Indeed, LIMK1 (or Kiz-1), a serine/threonine kinase containing two N-terminal LIM domains followed by a single PDZ motif that is strongly expressed in brain, has been recently implicated in impaired visuospatial constructive cognition in the developmental disorder Williams syndrome (Frangiskakis *et al.*, 1996). Also, for PDZ-containing proteins such as DlgA (Bryant *et al.*, 1993), Canoe (Miyamoto *et al.*, 1995), Dsh (Theisen *et al.*, 1994), and INAD (Shieh and Zhu, 1996) in *Drosophila* and LIN-2 (Hoskins *et al.*, 1996), LIN-7 (Simske

et al., 1996), and PAR3 (Etemad Moghadam *et al.*, 1995) in *Caenorhabditis elegans*, the severe impact of mutations on growth and differentiation has been documented. Further characterization of the exact topological and dynamic constraints that govern the interactive capacities of LIM and PDZ domains should therefore help us in understanding the molecular mechanisms underlying these defects.

ACKNOWLEDGMENTS

We thank Drs. Finley and Brent for providing the yeast interaction trap plasmids and yeast strain and Dr. Claude Sardet for the human G0-fibroblast cDNA library. We gratefully acknowledge Drs. Anne Debant and Michel Streuli for making us familiar with the two-hybrid interaction trap and for their kind hospitality during the initial phase of the project. This work was supported in part by a grant from the Dutch Cancer Society to W.H. and by a Dutch Cancer Society travel grant to H.G.

REFERENCES

Altschul, S.F., Gish, W., Miller, W., Myers, E.W., and Lipman, D.J. (1990). Basic local alignment search tool. J. Mol. Biol. *215*, 403–410.

Arber, S., and Caroni, P. (1996). Specificity of single LIM motifs in targeting and LIM/LIM interactions in situ. Genes Dev. *10*, 289–300.

Banville, D., Ahmad, S., Stocco, R., and Shen, S.H. (1994). A novel protein-tyrosine phosphatase with homology to both the cytoskeletal proteins of the band 4.1 family and junction-associated guanylate kinases. J. Biol. Chem. *269*, 22320–22327.

Boedigheimer, M., Bryant, P., and Laughon, A. (1993). Expanded, a negative regulator of cell proliferation in *Drosophila*, shows homology to the NF2 tumor suppressor. Mech. Dev. *44*, 83–84.

Bradford, M.M. (1976). A rapid and sensitive method for the quantitation of microgram quantities of protein utilizing the principle of protein-dye binding. Anal. Biochem. *72*, 248–254.

Brenman, J.E., *et al.* (1996). Interaction of nitric oxide synthase with the postsynaptic density protein PSD-95 and alpha1-syntrophin mediated by PDZ domains. Cell *84*, 757–767.

Bryant, P.J., Watson, K.L., Justice, R.W., and Woods, D.F. (1993). Tumor suppressor genes encoding proteins required for cell interactions and signal transduction in *Drosophila*. Development (suppl), 239–249.

Chida, D., Kume, T., Mukouyama, Y., Tabata, S., Nomura, N., Thomas, M.L., Watanabe, T., and Oishi, M. (1995). Characterization of a protein tyrosine phosphatase (RIP) expressed at a very early stage of differentiation in both mouse erythroleukemia and embryonal carcinoma cells. FEBS Lett. *358*, 233–239.

Cho, K.-O., Hunt, C.A., and Kennedy, M.B. (1992). The rat brain postsynaptic density fraction contains a homolog of the *Drosophila* discs-large tumor suppressor protein. Neuron *9*, 929–942.

Cohen, G.B., Ren, R., and Baltimore, D. (1995). Modular binding domains in signal transducing proteins. Cell *80*, 237–248.

Cuppen, E., Nagata, S., Wieringa, B., and Hendriks, W. (1997). No evidence for involvement of mouse protein-tyrosine phosphatase-BAS-like/Fas-associated phosphatase-1 in Fas-mediated apoptosis. J. Biol. Chem. *272*, 30215–30220.

Dawid, I.B., Toyama, R., and Taira, M. (1995). LIM domain proteins. Crit. Rev. Acad. Sci. *318*, 295–306.

Doyle, D.A., Lee, A., Lewis, J., Kim, E., Sheng, M., and MacKinnon, R. (1996). Crystal structures of a complexed and peptide-free membrane protein-binding domain: molecular basis of peptide recognition by PDZ. Cell *85*, 1067–1076.

Etemad Moghadam, B., Guo, S., and Kemphues, K.J. (1995). Asymmetrically distributed PAR-3 protein contributes to cell polarity and spindle alignment in early *C. elegans* embryos. Cell *83*, 743–752.

Fanning, A.S., and Anderson, J.M. (1996). Protein–protein interactions: PDZ domain networks. Curr. Biol. *6*, 1385–1388.

Feuerstein, R., Wang, X., Song, D., Cooke, N.E., and Liebhaber, S.A. (1994). The LIM/double zinc-finger motif functions as a protein dimerization domain. Proc. Natl. Acad. Sci. USA *91*, 10655–10659.

Frangioni, J.V., and Neel, B.G. (1993). Solubilization and purification of enzymatically active glutathione S-transferase (pGEX) fusion proteins. Anal. Biochem. *210*, 179–187.

Frangiskakis, J.M., *et al.* (1996). LIMK-1 hemizygosity implicated in impaired visuospatial constructive cognition. Cell *86*, 59–69.

Garner, C.C. (1996). Synaptic proteins and the assembly of synaptic junctions. Trends Cell Biol. *6*, 429–433.

Gomperts, S.N. (1996). Clustering membrane proteins: it's all coming together with the PSD-95/SAP90 protein family. Cell *84*, 659–662.

Green, S., Issemann, I., and Sheer, E. (1988). A versatile in vivo and in vitro eukaryotic expression vector for protein engineering. Nucleic Acids Res. *16*, 369.

Gyuris, J., Golemis, E., Chertkov, H., and Brent, R. (1993). Cdi1, a human G1 and S phase protein phosphatase that associates with Cdk2. Cell *75*, 791–803.

Hammarstrom, A., Berndt, K.D., Sillard, R., Adermann, K., and Otting, G. (1996). Solution structure of a naturally occurring zinc-peptide complex demonstrates that the N-terminal zinc-binding module of the Lasp-1 LIM domain is an independent folding unit. Biochemistry *35*, 12723–12732.

Harrison, S.C. (1996). Peptide-surface association: the case of PDZ and PTB domains. Cell *86*, 341–343.

Hendriks, W., Schepens, J., Bachner, D., Rijss, J., Zeeuwen, P., Zechner, U., Hameister, H., and Wieringa, B. (1995). Molecular cloning of a mouse epithelial protein-tyrosine phosphatase with similarities to submembranous proteins. J. Cell. Biochem. *59*, 418–430.

Hoskins, R., Hajnal, A.F., Harp, S.A., and Kim, S.K. (1996). The *C. elegans* vulval induction gene *lin-2* encodes a member of the MAGUK family of cell junction proteins. Development *122*, 97–111.

Hunter, T. (1995). Protein kinases and phosphatases: the yin and yang of protein phosphorylation and signaling. Cell *80*, 225–236.

Inazawa, J., Ariyama, T., Abe, T., Druck, T., Ohta, M., Huebner, K., Yanagisawa, J., Reed, J.C., and Sato, T. (1996). PTPN13, a Fas-associated protein tyrosine phosphatase, is located on the long arm of chromosome 4 at band q21.3. Genomics *31*, 240–242.

Kiess, M., Scharm, B., Aguzzi, A., Hajnal, A., Klemenz, R., Schwarte Waldhoff, I., and Schafer, R. (1995). Expression of RIL, a novel LIM domain gene, is down-regulated in Hras-transformed cells and restored in phenotypic revertants. Oncogene *10*, 61–68.

Kim, E., Niethammer, M., Rothschild, A., Jan, Y.N., and Sheng, M. (1995). Clustering of Shaker-type K+ channels by interaction with a family of membrane-associated guanylate kinases. Nature *378*, 85–88.

Kornau, H.C., Schenker, L.T., Kennedy, M.B., and Seeburg, P.H. (1995). Domain interaction between NMDA receptor subunits and the postsynaptic density protein PSD-95. Science *269*, 1737–1740.

Lemmon, M.A., Ferguson, K.M., and Schlessinger, J. (1996). PH domains: diverse sequences with a common fold recruit signaling molecules to the cell surface. Cell *85*, 621–624.

Maekawa, K., Imagawa, N., Nagamatsu, M., and Harada, S. (1994). Molecular cloning of a novel protein-tyrosine phosphatase containing a membrane-binding domain and GLGF repeats. FEBS Lett. *337*, 200–206.

Mauro, L.J., and Dixon, J.E. (1994). "Zip codes" direct intracellular protein tyrosine phosphatases to the correct cellular "address." Trends Biochem. Sci. *19*, 151–155.

Miyamoto, H., Nihonmatsu, I., Kondo, S., Ueda, R., Togashi, S., Hirata, K., Ikegami, Y., and Yamamoto, D. (1995). Canoe encodes a novel protein containing a GLGF/DHR motif and functions with notch and scabrous in common developmental pathways in *Drosophila*. Genes Dev. *9*, 612–625.

Morais Cabral, J.H., Petrosa, C., Sutcliffe, M.J., Raza, S., Byron, O., Poy, F., Marfatia, S.M., Chishti, A.H., and Liddington, R.C. (1996). Crystal structure of a PDZ domain. Nature *382*, 649–652.

Niethammer, M., Kim, E., and Sheng, M. (1996). Interaction between the C terminus of NMDA receptor subunits and multiple members of the PSD-95 family of membrane-associated guanylate kinases. J. Neurosci. *16*, 2157–2163.

Okano, I., Hiraoka, J., Otera, H., Nunoue, K., Ohashi, K., Iwashita, S., Hirai, M., and Mizuno, K. (1995). Identification and characterization of a novel family of serine/threonine kinases containing two N-terminal LIM motifs. J. Biol. Chem. *270*, 31321–31330.

Pawson, T. (1995). Protein modules and signalling networks. Nature *373*, 573–580.

Perez Alvarado, G.C., Kosa, J.L., Louis, H.A., Beckerle, M.C., Winge, D.R., and Summers, M.F. (1996). Structure of the cysteine-rich intestinal protein, CRIP. J. Mol. Biol. *257*, 153–174.

Ponting, C.P., and Phillips, C. (1995). DHR domains in syntrophins, neuronal NO synthases and other intracellular proteins. Trends Biochem. Sci. *20*, 102–103.

Saras, J., Claesson Welsh, L., Heldin, C.H., and Gonez, L.J. (1994). Cloning and characterization of PTPL1, a protein tyrosine phosphatase with similarities to cytoskeletal-associated proteins. J. Biol. Chem. *269*, 24082–24089.

Saras, J., Engström, U., Gonez, L.J., and Heldin, C.H. (1997a). Characterization of the interactions between PDZ domains of the protein-tyrosine phosphatase PTPL1 and the carboxyl-terminal tail of Fas. J. Biol. Chem. *272*, 20979–20981.

Saras, J., Franzen, P., Aspenstrom, P., Hellman, U., Gonez, L.J., and Heldin, C.H. (1997b). A novel GTPase-activating protein for Rho interacts with a PDZ domain of the protein-tyrosine phosphatase PTPL1. J. Biol. Chem. *272*, 24333–24338.

Sato, T., Irie, S., Kitada, S., and Reed, J.C. (1995). FAP-1: a protein tyrosine phosphatase that associates with Fas. Science *268*, 411–415.

Schepens, J., Cuppen, E., Wieringa, B., and Hendriks, W. (1997). The neuronal nitric oxide synthase PDZ motif binds to −GDXV* carboxyterminal sequences. FEBS Lett. *409*, 53–56.

Schwartz, R.M., and Dayhoff, M.O. (1979). In: Atlas of Protein Sequence and Structure, ed. M.O. Dayhoff, Washington, DC: National Biomedical Research Foundation, 353–358.

Serra Pages, C., Kedersha, N.L., Fazikas, L., Medley, Q., Debant, A., and Streuli, M. (1995). The LAR transmembrane protein tyrosine phosphatase and a coiled-coil LAR-interacting protein co-localize at focal adhesions. EMBO J. *14*, 2827–2838.

Shieh, B.H., and Zhu, M.Y. (1996). Regulation of the TRP Ca2+ channel by INAD in *Drosophila* photoreceptors. Neuron *16*, 991–998.

Simske, J.S., Kaech, S.M., Harp, S.A., and Kim, S.K. (1996). LET-23 receptor localization by the cell junction protein LIN-7 during *C. elegans* vulval induction. Cell *85*, 195–204.

Songyang, Z., and Cantley, L.Z. (1995). Recognition and specificity in protein tyrosine kinase mediated signalling. Trends Biochem. Sci. *20*, 470–475.

Songyang, Z., Fanning, A.S., Fu, C., Xu, J., Marfatia, S.M., Chishti, A.H., Crompton, A., Chan, A.C., Anderson, J.M., and Cantley, L.C. (1997). Recognition of unique carboxyl-terminal motifs by distinct PDZ domains. Science *275*, 73–77.

Stricker, N.L., Christopherson, K.S., Yi, B.A., Schatz, P.J., Raab, R.W., Dawes, G., Bassett, D.E., Bredt, D.S., and Li, M. (1997). PDZ domain of neuronal nitric oxide synthase recognizes novel C-terminal peptide sequences. Nature Biotech. *15*, 336–342.

Theisen, H., Purcell, J., Bennett, M., Kansagara, D., Syed, A., and Marsh, J.L. (1994). *Dishevelled* is required during *wingless* signaling to establish both cell polarity and cell identity. Development *120*, 347–360.

Tsukita, S., Itoh, M., Nagafuchi, A., Yonemura, S., and Tsukita, S. (1993). Submembranous junctional plaque proteins include potential tumor suppressor molecules. J. Cell Biol. *123*, 1049–1053.

van den Maagdenberg, A.M., Olde Weghuis, D., Rijss, J., Merkx, G.F., Wieringa, B., Geurts van Kessel, A., and Hendriks, W.J. (1996). The gene (PTPN13) encoding the protein tyrosine phosphatase PTP-BL/PTP-BAS is located in mouse chromosome region 5E/F and human chromosome region 4q21. Cytogenet. Cell Genet. *74*, 153–155.

Wang, H., Harrison Shostak, D.C., Lemasters, J.J., and Herman, B. (1995). Cloning of a rat cDNA encoding a novel LIM domain protein with high homology to rat RIL. Gene *165*, 267–271.

Woods, D.F., and Bryant, P.J. (1993). ZO-1, DlgA and PSD-95/SAP90: homologous proteins in tight, septate and synaptic cell junctions. Mech. Dev. *44*, 85–89.

Woods, D.F., Hough, C., Peel, D., Callaini, G., and Bryant, P.J. (1996). Dlg protein is required for junction structure, cell polarity, and proliferation control in *Drosophila* epithelia. J. Cell Biol. *134*, 1469–1482.

Wu, R.Y., and Gill, G.N. (1994). LIM domain recognition of a tyrosine-containing tight turn. J. Biol. Chem. *269*, 25085–25090.

Xia, H., Winokur, S.T., Kuo, W., Altherr, M.R., and Bredt, D.S. (1997). Actinin-associated LIM protein: identification of a domain interaction between PDZ and spectrin-like repeat motifs. J. Cell Biol. *139*, 507–515.